

## ATMOSPHERIC IMAGING ASSEMBLY OBSERVATIONS OF HOT FLARE PLASMA

KATHARINE K. REEVES AND LEON GOLUB

Harvard-Smithsonian Center for Astrophysics, 60 Garden St. MS 58, Cambridge, MA 02138, USA; [kreeves@cfa.harvard.edu](mailto:kreeves@cfa.harvard.edu)

Received 2010 November 9; accepted 2010 December 20; published 2011 January 13

### ABSTRACT

We present observations of hot plasma from solar eruptions recorded by the Atmospheric Imaging Assembly (AIA) on the *Solar Dynamics Observatory*. AIA is the first narrowband instrument capable of taking images of hot plasma in the 5–15 MK range. We find that there are hot structures above flare loops, and that they are typically more diffuse and nebulous than the well-defined flare loops. Because of the narrowband response, high sensitivity, and high spatial resolution of AIA, these supra-arcade structures are visible in exquisite detail, particularly in the 131 Å and 94 Å channels. In one event, a C4.9 flare observed on 2010 November 3, hot plasma is seen to outline an erupting plasmoid and possibly a current sheet. We compare hot plasma observed with AIA to structures observed with the X-Ray Telescope on the *Hinode* mission and find that the plasma imaged in AIA contains more fine detail. These new AIA observations show that supra-arcade flare structures and coronal mass ejections are highly structured not only in space and time, but also in temperature. This thermal structuring is expected, based on modeling efforts, but has now been imaged directly for the first time over a large range of temperatures.

**Key words:** Sun: activity – Sun: coronal mass ejections (CMEs) – Sun: flares

*Online-only material:* animations

### 1. INTRODUCTION

Reconnection is widely accepted as the process that powers solar flares. One consequence of the reconnection process is hot plasma in the region of reconnection and in the post-flare loops. This plasma has been studied previously in the *Transition Region and Coronal Explorer (TRACE)* 195 Å passbands, since this channel contains Fe XXIV with a formation temperature of 20 MK, as well as cooler Fe XII plasma formed at 1.5 MK (Warren et al. 1999; Warren 2000; Warren & Reeves 2001). Recently, observations of hot plasma in a current sheet-like structure were reported by Savage et al. (2010), who analyzed observations in the soft X-rays. These regions of hot plasma often show interesting dynamics, such as dark voids flowing down toward the post-flare arcade (McKenzie & Hudson 1999; McKenzie 2000; Innes et al. 2003a, 2003b; McKenzie & Savage 2009).

Until now, hot flare plasma has primarily been imaged by either the *TRACE* 195 Å channel, or broadband X-ray imagers such as the soft X-ray telescope (SXT) on the *Yohkoh* mission, or the X-Ray Telescope (XRT) on the *Hinode* mission. The Atmospheric Imaging Assembly (AIA; Lemen et al. 2010) on the *Solar Dynamics Observatory* offers a completely new look at the hot plasma in flares. AIA has six narrowband EUV passbands that are sensitive to different ionization states of iron. The 193 Å channel, similar to the *TRACE* 195 Å channel, contains lines from both Fe XXIV and Fe XII. In flares, the 131 Å channel primarily contains contributions from Fe XXI, formed at 11 MK. The 94 Å channel contains lines from Fe X, formed at 1 MK, and Fe XVIII, formed at 7 MK. The 335 Å channel mainly contains contributions from Fe XVI, formed at 2.5 MK. The 211 Å channel contains mostly Fe XIV, formed at 2 MK, and the 171 Å channel contains mostly Fe IX, formed at 0.6 MK (see O’Dwyer et al. 2010, for detailed information about line contributions to the AIA channels). This broad temperature coverage allows for an unprecedented look at the thermal structure in solar eruptions.

### 2. OBSERVATIONS

AR 11121 was observed at the limb on 2010 November 3–5. Observations were taken in several AIA wavebands at a cadence

of about 12 s, with a resolution of  $\sim 0.6''$  per pixel. Several flares occurred during this time, including a C4.9 flare that peaked at 12:21 UT on November 3, an M1.6 flare that peaked at 23:58 on November 4, and an M1.0 flare that peaked at 13:29 UT on November 5. The light curves for these flares from the *GOES* 1–8 Å channel are shown in Figure 1.

The XRT (Golub et al. 2007) on *Hinode* also observed several of the flares from AR 11121. Observations were taken in the Al-mesh, Ti-poly, Thick Al, and Thick Be filters with a cadence of about 30 s. The thin filters, Al-mesh and Ti-poly, have peak temperature responses at  $\sim 8$  MK and  $\sim 10$  MK, respectively. The thick filters, Thick Al and Thick Be, both have peak temperatures at  $\sim 13$  MK, but the Thick Al response allows for imaging of cooler plasma than the Thick Be filter. We have reported the peak temperatures of the XRT filter response functions, but these filters are able to detect a wide range of temperatures because of their broad responses (see Narukage et al. 2011, for details of the XRT calibration and filter response functions). The thick filters observed the flaring region with a field of view of  $\sim 384'' \times 384''$  and a resolution of  $\sim 1''$  per pixel. The thin filter observations have a field of view of  $\sim 512'' \times 512''$  and a resolution of  $\sim 2''$  per pixel.

The M1.0 flare that occurred on 2010 November 5 provides a good example of hot flare plasma as seen in the AIA passbands. Images from all six AIA EUV passbands are shown in Figure 2 at around 13:48 UT, about 20 minutes after the peak of the flare in the *GOES* 1–8 Å channel. There is clearly a large structure seen in the 131 Å and 94 Å channels above the flare loops. This structure is diffuse and it has a nebulous morphology, in contrast to the bright, well-defined post-flare loops that are also seen in these channels during the flare.

At 13:48 UT, the other four channels shown in Figure 2 show very little evidence of the structures that are clearly visible in the 94 Å and 131 Å channels. Thus, the supra-arcade emission is likely to be above about 5 MK, since it is not visible in the 335 Å channel, and it is probably below about 18 MK, since it is not visible in the 193 Å channel. As the structure evolves and fades in the hot channels, some similar structures begin to appear in the 335 Å, 211 Å, and 193 Å channels, but especially

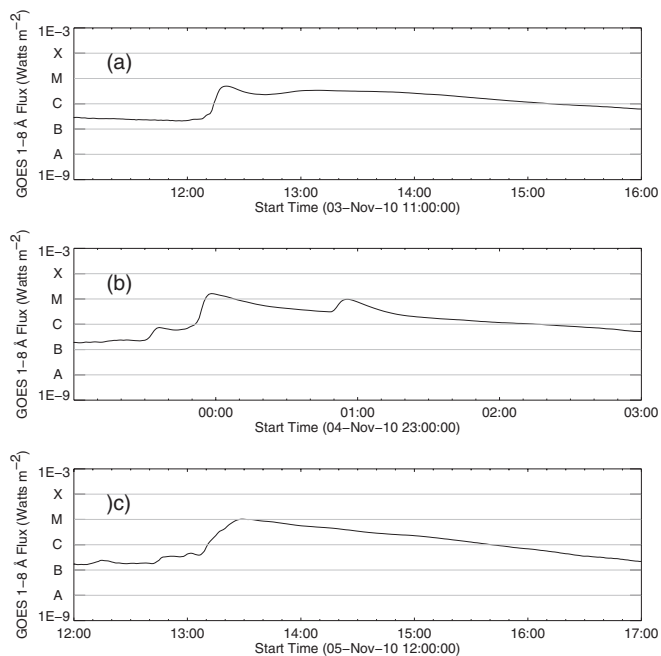


**Figure 1.** Plots of the *GOES* 1–8 Å flux for the three flares discussed in this Letter. (a) C4.9 flare on November 3, (b) M1.6 flare on November 4, and (c) M1.0 flare on November 5.

in the case of the 211 Å and 193 Å channels, these structures are difficult to discern from the background emission (see the animation associated with Figure 2). No evidence for the supra-arcade structure is seen at all in the 171 Å channel.

The C4.9 flare that occurred on 2010 November 3 is an interesting example of hot plasma observations because it shows hot signatures in the erupting plasmoid itself. AIA observations in the hot channels (131 Å, 94 Å, and 335 Å) from this flare are shown for three different times in Figure 3. This flare was partially occulted by the limb. A few minutes before the peak of the flare, at 12:15 UT, an eruption is clearly seen in the hot channels. A circular structure appears bright in the 131 Å, and can be seen, albeit fainter, in the 94 Å channel as well. In the 335 Å channel, a faint structure can be seen outlining the erupting plasma.

A few minutes later in the eruption, at 12:23 UT, a long thin structure is clearly visible in the 131 Å image, and faint indications of this structure are also seen in the 94 Å and 335 Å images. This structure is reminiscent of the “current sheet candidate” found in XRT data of an eruption by Savage et al. (2010). The dynamics of this event indicate that this structure is connected to the erupting plasmoid (see the animation associated with Figure 3), and may be indicative of a current sheet, or at the very least, hot structures surrounding the current sheet.

Later in the flare evolution, diffuse structures form above the flare arcade, as in the M1.0 flare discussed previously. These structures are visible in all three of the hot channels, though they are most visible in the 131 Å channel, as can be seen in the bottom row of Figure 3. These structures have a complicated morphology, and they evolve quickly, especially around the edges furthest away from the Sun’s surface.

The M1.6 flare that peaked at 23:58 UT on 2010 November 4 also has accompanying XRT data and is useful for comparing the hot plasma imaged in narrowband and broadband imagers. AIA and XRT observations from this flare are shown in Figure 4.

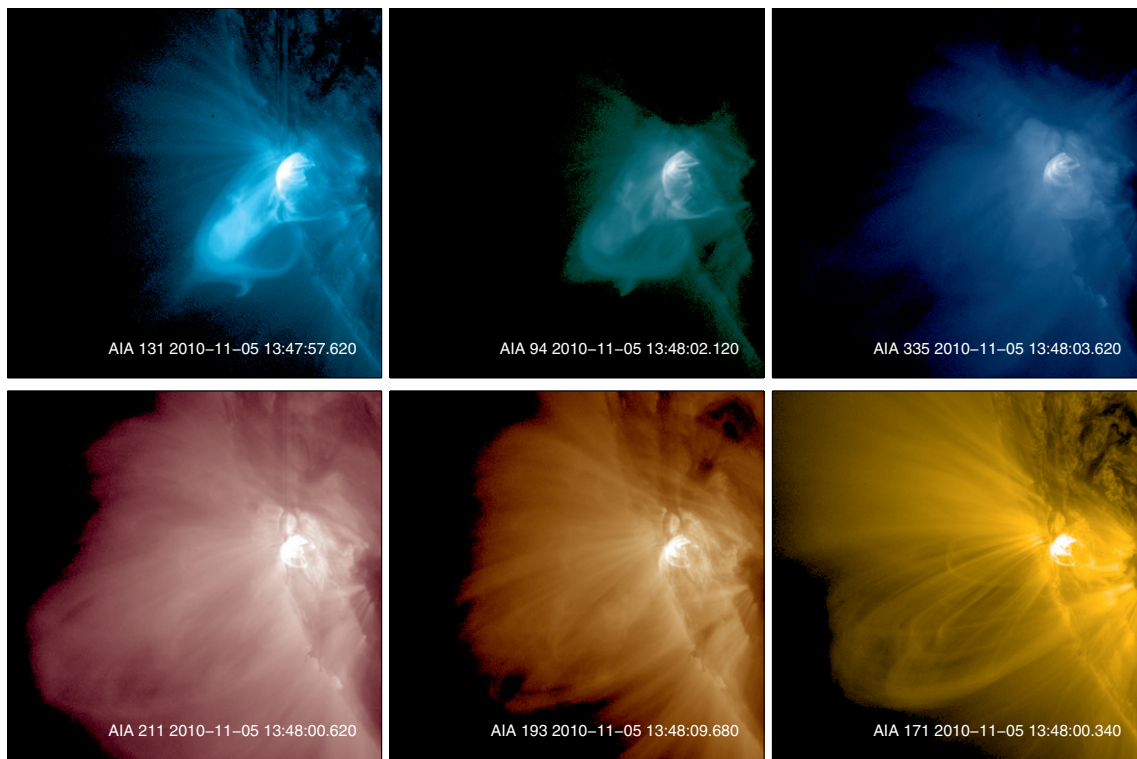


**Figure 2.** AIA and XRT observations of an M1.0 flare on 2010 November 5. Top row: AIA 131 Å (11 MK) (left), AIA 94 Å (7 MK) (center), and AIA 335 Å (2.5 MK) (right). Bottom row: AIA 211 Å (2 MK) (left), AIA 193 Å (20 MK, 1.3 MK) (center), and AIA 171 Å (0.6 MK) (right). The field of view for all the images is about 460'' × 460''.

(An animation of this figure is available in the online journal.)

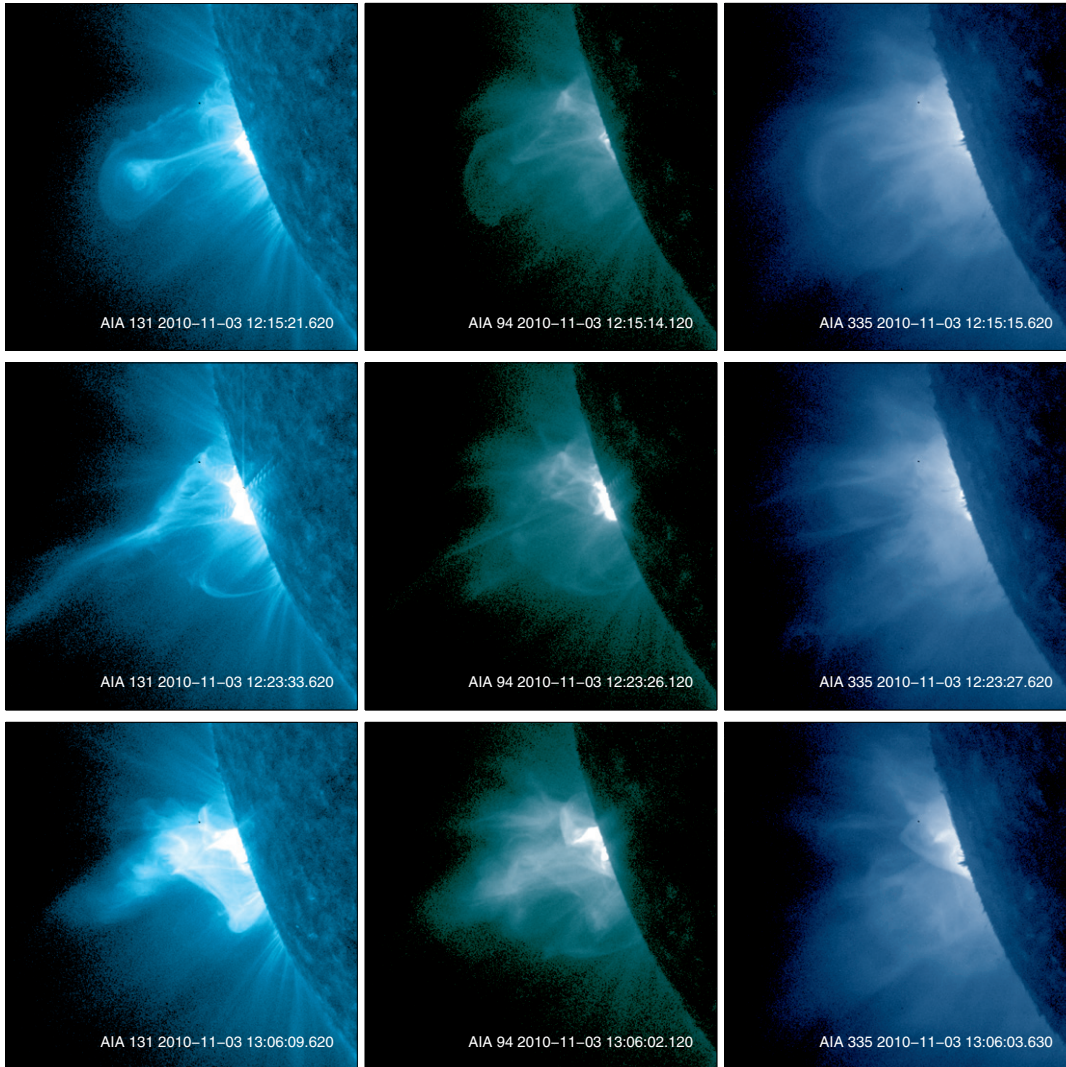


**Figure 3.** AIA observations of a C4.9 flare on 2010 November 3. Top row: AIA 131 Å (11 MK) (left), AIA 94 Å (7 MK) (center), and AIA 335 Å (2.5 MK) (right) at about 12:15 UT. Middle row: Same AIA filters, taken at about 12:23 UT. Bottom row: Same AIA filters, taken at about 13:06 UT. The field of view for all the images is about  $460'' \times 460''$ .

(An animation of this figure is available in the online journal.)

At the time shown in the figure, there are clear, bright structures above the flare loops in the 94 Å and the 131 Å channels, but no clear indication of a corresponding structure in the 335 Å channel. As with the M1.0 flare on November 5, this structure is diffuse and nebulous. The same structure is also seen in the XRT images, though with less definition. The resolution and narrow temperature response of AIA allows for rendering the details of these hot structures in exquisite detail, while the broadband image from XRT shows all of the hot plasma.

The structures above the flare loops are brightest in the AIA images about 30 minutes after the peak of the flare in the *GOES*. As the flare evolves, the southeasterly tip of this structure exhibits dynamic and turbulent fluid-like motions (see the animation associated with Figure 4). At about 1:00 UT, structures overlying the loops begin to be visible in the 335 Å channel, indicating that the supra-arcade structure is cooling down into the 335 Å passband.

### 3. FLARE SIMULATIONS

In Figure 5, we show simulated AIA flare emission calculated using the MAS (MHD Around a Sphere) code developed by

Predictive Sciences, Inc. (e.g., Mikić et al. 1999; Linker et al. 2001, 2003; Lionello et al. 2009). The model solves the MHD equations in 2.5 dimensions in spherical coordinates, including conduction and radiation in the energy equation. This simulation is the same as the one reported in Reeves et al. (2010), and more details on the initial conditions, boundary conditions, and methods of solution can be found there. This simulation is not meant to exactly simulate any of the observed flares, but rather to help guide our understanding of the structures that are seen in the observations.

In Figure 5, emission is clearly seen in the current sheet structure in the AIA 131 and 94 channels. The current sheet in the simulation is at  $\sim 6\text{--}10$  MK, putting it right in the range of temperatures where the 94 Å and 131 Å channels are the most sensitive. Thus, the simulation provides a possible explanation for the supra-arcade plasma, i.e., that it is associated with the hot structures surrounding the current sheet. The simulation has a simple 2.5-dimensional geometry, and of course cannot reproduce the complexity of the observations, but it does indicate a possible interpretation for the hot plasma.

All of the AIA channels show an intensity enhancement in the area just outside of the current sheet in the simulations.

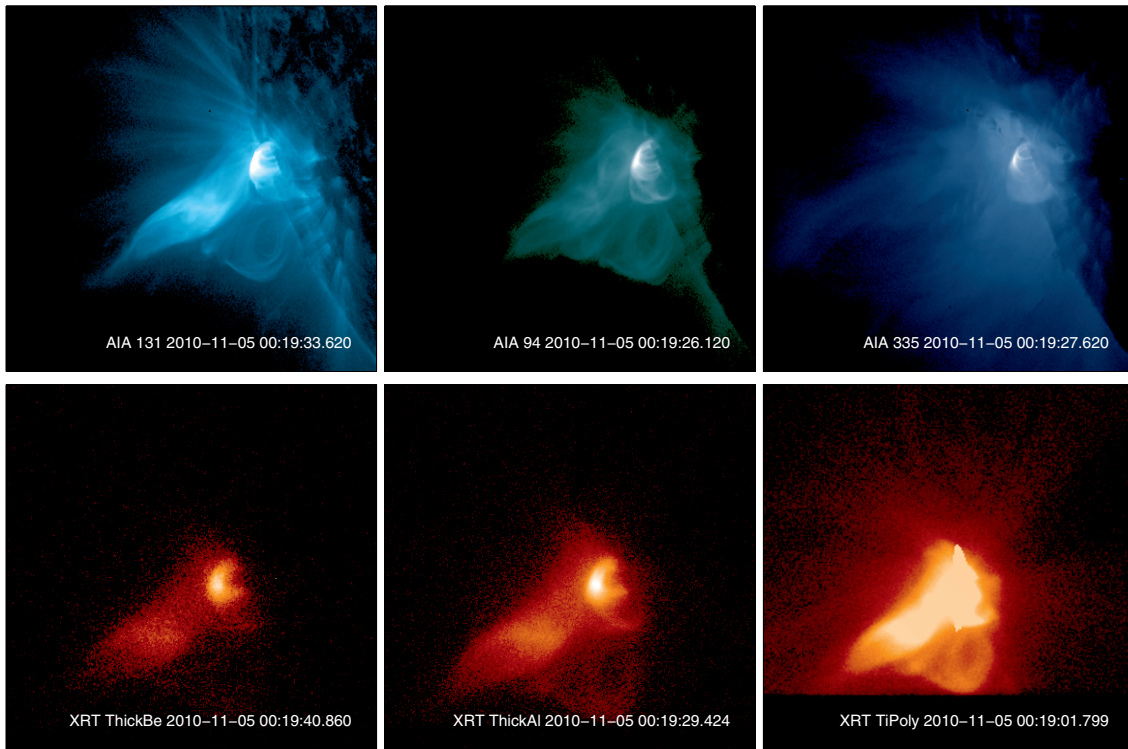


**Figure 4.** AIA and XRT observations of an M1.6 flare that peaked at 23:58 UT on 2010 November 4. Top row: AIA 131 Å (11 MK) (left), AIA 94 Å (7 MK) (center), and AIA 335 Å (2.5 MK) (right). Bottom row: XRT Thick Be (left), XRT Thick Al (center), and XRT Ti-poly (right). The XRT Al-mesh filter is not shown due to saturation. The field of view for the AIA images is about  $460 \times 460''$ . The field of view is about  $384'' \times 384''$  for the thick XRT filters and  $512'' \times 512''$  for the XRT Ti-poly filter.

(An animation of this figure is available in the online journal.)

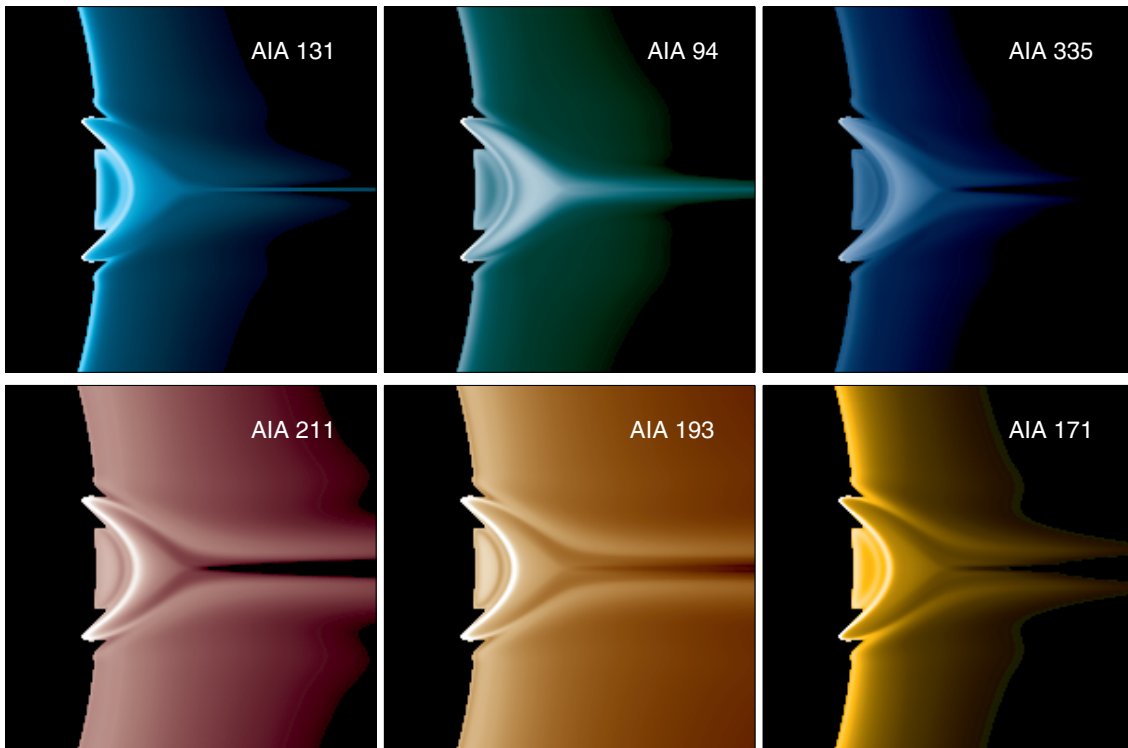


**Figure 5.** Simulated AIA flare observations. Top row: AIA 131 Å (left), AIA 94 Å (center), and AIA 335 Å (right). Bottom row: AIA 211 Å (left), AIA 193 Å (center), and AIA 171 Å (right).

This effect happens because conduction in the current sheet causes hot plasma to spread out of the current sheet region, forming a thermal halo (Reeves et al. 2010). This effect has been

seen previously in other MHD flare simulations (Yokoyama & Shibata 1997) and analytical calculations of reconnection including conduction (Seaton & Forbes 2009). The simulated

images in Figure 5 have been scaled so that all the plasma is visible. In reality, the plasma around the current sheet would be quite difficult to see in the 171 Å passband since the current sheet structures are five orders of magnitude more faint than the flare loops.

#### 4. DISCUSSION AND CONCLUSIONS

This Letter reports the first narrowband imaging of hot plasma at 131 Å, 94 Å, and 335 Å in solar eruptions. In these passbands, we clearly see structures above the flare arcade that are diffuse and nebulous, though also containing significant detail. These structures are probably the same as the “fan arcades” seen above solar flares in SXT observations (e.g., Švestka et al. 1998; McKenzie & Hudson 1999), but because of the high spatial resolution and narrowband temperature response, AIA images this plasma in much finer detail than broadband imagers such as SXT or XRT. These supra-arcade structures are probably in regions of weak magnetic field surrounding the current sheet, allowing their morphology to be more diffuse than the post-flare loops, which occur in strong field regions.

We have shown that these supra-arcade structures are imaged particularly well in the AIA 131 Å and 94 Å bandpasses. There have been a few examples of bright supra-arcade structures imaged in X-class flares in the 195 Å passband of *TRACE*, most famously the X1.5 flare of 2002 April 21 (Innes et al. 2003a, 2003b). These structures are generally assumed to be visible in the *TRACE* 195 Å passband due to Fe xxiv, which has a formation temperature of about 20 MK. Since the AIA 131 Å channel images flare plasma at about 11 MK and the 94 Å channel images flare plasma at about 7 MK, these two AIA wavebands are able to observe plasma at cooler temperatures than the hot contribution to the *TRACE* 195 Å channel. It could be that supra-arcade structures observed by 195 Å channels were previously rare because few flares reach the high temperatures needed to form the Fe xxiv above the flare arcade. Additionally, the high-temperature contribution to the 131 Å and 94 Å channels is a major component of the response in these passbands, unlike the 195 Å *TRACE* channel, which has a strong contribution from Fe xii. Thus, the hot AIA channels do not have cooler flare material interfering with the imaging of the hot supra-arcade plasma, rendering the images of the hot plasma incredibly clear and sharp.

The fact that we see the supra-arcade in several flares indicates that this plasma is a general feature of eruptions, and not just a peculiarity of one event. Since this plasma is imaged with great clarity and detail in the 131 Å and 94 Å AIA channels,

we expect that these observations will lead to fruitful advances in understanding flare physics. We are currently examining the November 3 flare in more detail in light of the model presented above and will present the results in a forthcoming paper.

Our results clearly show that erupting plasmoids and supra-arcade flare structures consist of plasma at many different temperatures. It seems likely that this thermal structuring extends into the outer corona as coronal mass ejections (CMEs) erupt. Thus, EUV imaging of the corona could provide fruitful results for further CME research.

The authors thank the anonymous referee, who provided useful comments that improved the Letter. K.K.R. is partially supported under the NSF-SHINE program, grant number ATM0752257. K.K.R. and L.G. are both supported under contract SP02H1701R from Lockheed-Martin to SAO and contract NNM07AB07C from NASA to SAO. *Hinode* is a Japanese mission developed and launched by ISAS/JAXA, with NAOJ as domestic partner and NASA and STFC (UK) as international partners. It is operated by these agencies in cooperation with ESA and NSC (Norway).

#### REFERENCES

- Golub, L., et al. 2007, *Sol. Phys.*, **243**, 63  
 Innes, D. E., McKenzie, D. E., & Wang, T. 2003a, *Sol. Phys.*, **217**, 267  
 Innes, D. E., McKenzie, D. E., & Wang, T. 2003b, *Sol. Phys.*, **217**, 247  
 Lemen, J. R., et al. 2010, *Sol. Phys.*, submitted  
 Linker, J. A., Lionello, R., Mikić, Z., & Amari, T. 2001, *J. Geophys. Res.*, **106**, 25165  
 Linker, J. A., Mikić, Z., Lionello, R., Riley, P., Amari, T., & Odstrčil, D. 2003, *Phys. Plasmas*, **10**, 1971  
 Lionello, R., Linker, J. A., & Mikić, Z. 2009, *ApJ*, **690**, 902  
 McKenzie, D. E. 2000, *Sol. Phys.*, **195**, 381  
 McKenzie, D. E., & Hudson, H. S. 1999, *ApJ*, **519**, L93  
 McKenzie, D. E., & Savage, S. L. 2009, *ApJ*, **697**, 1569  
 Mikić, Z., Linker, J. A., Schnack, D. D., Lionello, R., & Tarditi, A. 1999, *Phys. Plasmas*, **6**, 2217  
 Narukage, N., et al. 2011, *Sol. Phys.*, in press (arXiv:1011.2867)  
 O’Dwyer, B., Del Zanna, G., Mason, H. E., Weber, M. A., & Tripathi, D. 2010, *A&A*, **521**, A21  
 Reeves, K. K., Linker, J. A., Mikić, Z., & Forbes, T. G. 2010, *ApJ*, **721**, 1547  
 Savage, S. L., McKenzie, D. E., Reeves, K. K., Forbes, T. G., & Longcope, D. W. 2010, *ApJ*, **722**, 329  
 Seaton, D. B., & Forbes, T. G. 2009, *ApJ*, **701**, 348  
 Švestka, Z., Fárnik, F., Hudson, H. S., & Hick, P. 1998, *Sol. Phys.*, **182**, 179  
 Warren, H. P. 2000, *ApJ*, **536**, L105  
 Warren, H. P., Bookbinder, J. A., Forbes, T. G., Golub, L., Hudson, H. S., Reeves, K., & Warshall, A. 1999, *ApJ*, **527**, L121  
 Warren, H. P., & Reeves, K. K. 2001, *ApJ*, **554**, L103  
 Yokoyama, T., & Shibata, K. 1997, *ApJ*, **474**, L61